Distinct Color Change of a Ho(III)-based Metal-Organic Framework upon Varying Incident Light Sources

Monu Joy, 1‡ Okan Zafer Yeşilel, 2‡ Mario Wriedt1*

¹Department of Chemistry and Biochemistry, The University of Texas at Dallas, Richardson, TX 75080, United States

²Department of Chemistry, Faculty of Science and Letters, Eskişehir Osmangazi University, 26040, Eskişehir, Turkey

[‡]MJ and OZY contributed equally to this work.

*Correspondence: Mario.Wriedt@UTDallas.edu

Abstract

Lanthanide metal-organic frameworks (Ln-MOFs) have gained significant attention in recent years due to their diverse characteristics ranging from material science to biomedical applications. Although Ln-MOFs possess properties that are common to all MOF categories, they can exhibit unique structural combinations owing to their high coordination numbers and distinctive optical properties. Herein, we report the Ho(III)-based zwitterionic MOF H1 which crystallizes in the monoclinic space group C2/c. The nine-coordinate Ho(III) ion presents a configuration related to the *gek2* topology. Remarkably, H1 features unique optical properties, namely, the physical change of color from white to pink upon changing the incident light source from sunlight to fluorescent light. A literature review through the Cambridge crystallographic data center (CCDC) reveals this being the first report of a Ho(III)-MOF showing such optical behavior.

1. Introduction

MOFs are nanoporous crystalline materials which are typically constructed by the coordination of metal ions or clusters with polytypic organic ligands. Their key properties including high surface areas and pore volumes are purely dependent on their architectures, determined by their building blocks and respective functionalities. Judicious control of the MOF structure can lead to materials suitable for defined applications.^{1,2} The design of Ln-MOFs has not only gained significant attention due their intriguing topologies but also for potential applications such as luminescence, magnetism, proton transport, sensing, catalysis, drug delivery and cancer therapy etc.^{3–15} One of the most attractive features of Ln-MOFs is the high coordination number, as it can self-assemble to form diverse geometries/topologies. Moreover, the synthesis of Ln-MOFs is a growing area in MOF research due to the properties mainly imparted by the lanthanide elements, especially for luminescence-based applications resulting from their 4f electronic shell.^{16–18} However, the generation of open metal sites in such MOFs and the probing of their potentially interesting adsorption properties continues to be a challenge as the removal of the coordinated solvent is often accompanied by framework deformation or collapse.^{19,20} Although investigations on the design and

characterization of Ln-MOFs are ongoing for about two decades, the number reported Ho(III)-MOFs is very limited to date. ^{21,22} For example, in 2021, Juan *et al.* reported the Ho analogue of UiO-66²³ and Maria *et al.* proposed an effective excitation mechanism for the emission of Ho(III)-based compounds that can result from an enhanced green luminescence with ${}^5S_2 \rightarrow {}^5I_8$ transition. ²⁴ Since lanthanide ions have relatively high affinities to ligands composed of oxygen-nitrogen heteroatom system, zwitterionic (ZW) ligands featuring a combination of pyridinium and carboxylate functionalities might be excellent candidates for new Ln-MOF discovery.

2. Experimental

2.1 Synthesis

The ligand 4-carboxy-1-(4-carboxybenzyl)-pyridinium bromide was synthesized as reported before.²⁵ The MOF was synthezised from stirring a mixture of Ho(NO₃)₃·6H₂O (43.4 mg, 0.10 mmol) and 4-carboxy-1-(4-carboxybenzyl)-pyridinium bromide (20.3 mg, 0.06 mmol) at room temperature in 5 mL of DMF-water-ethanol (1:1:1, 3 mL) for 30 min. The resulting solution was sealed in a glass vial and heated at 80 °C for 3 days to obtain pale pink crystals.

2. 2 Single crystal X-ray crystallography & CCDC literature search

Data collections were performed on single crystals coated with Paratone-N oil and mounted on Kapton loops. Single crystal X-ray data was collected on a Bruker Kappa Apex II X-ray diffractometer outfitted with a Mo X-ray source (sealed tube, $\lambda = 0.71073$ Å) and an APEX II CCD detector equipped with an Oxford Cryosystems Desktop Cooler low-temperature device. The APEX-II software suite was used for data collection, cell refinement, and reduction. Absorption corrections were applied using SADABS.²⁶ Space group assignments were determined by examination of systematic absences, E-statistics, and successive refinement of the structures. Structure solutions were performed with direct methods using SHELXT²⁷ and structure refinements were performed by least-squares refinement against $|F|^2$ followed by difference Fourier synthesis using SHELXL.²⁸ All non-hydrogen atoms were refined with anisotropic displacement parameters. The C-H atoms were positioned with idealized geometry and were refined with fixed isotropic displacement parameters $[U_{eq}(H) = -1.2U_{eq}(C)]$ using a riding model with $d_{C-H} = 0.95$ Å (aromatic). The data were corrected using the SQUEEZE option in PLATON.²⁹ CCDC 2254030 contains the supplementary crystallographic data for this paper. These data can be obtained free of charge from the Cambridge Crystallographic Data Centre via www.ccdc.cam.ac.uk. Selected crystal data and details on structure determinations are listed in Table S1. The CCDC search for Holmium MOFs was based on CCDC MOF-subset version 2022. Conquest 2022.3.0³⁰ software was used to collect the structural data listed in Table S3.

2.3 Other characterizations

Powder X-ray diffraction data was collected at room temperature using a Bruker D2 Phaser diffractometer equipped with a Cu-sealed tube (λ = 1.54178 Å). The powder samples were spread on low-background discs for analysis. Thermogravimetric analysis was performed using a Perkin Elmer Diamond TG/DTA thermal analyzer under a static air atmosphere from 30 to 800 °C. The UV–vis spectrum was collected using an Agilent Cary 60 spectrophotometer. The photoluminescence emission spectrum was obtained under different excitation wavelengths using a PerkinElmer LS-55 spectrophotometer.

3. Result and discussion

3.1 Chemistry and crystallization

4-carboxy-1-(4-carboxybenzyl)-pyridinium bromide (H₂LBr) is a flexible ditopic ZW ligand that is known to form ZW-MOFs with interesting non-covalent interactions and diverse structural topologies. Herein, the reaction of H₂LBr with Ho(NO₃)₃·6H₂O in a trinary solvent system (DMF, water and ethanol) resulted in the growth of pink colored and block-shaped single crystals of H1. Single crystal X-ray structural analysis revealed a composition of [Ho(μ_4 -L)(μ_1 , μ_2 -CHOO)(μ_2 -NO₃)]_n. Figure 1a and 1b shows the metal coordination environment and crystal packing of this MOF, respectively. Phase purity of the bulk sample was confirmed by powder X-ray diffraction as represented in Figure 2a.

3.2 Crystallographic description

H1 crystallizes in a monoclinic crystal system with space group C2/c. Table S1 lists associated structural data and refinement details. The asymmetric unit contains one MOF equivalent composed of one Ho(III) cation and ZW ligand, and one nitrate and formate anion with all atoms located in crystallographically independent positions. The crystal lattice contains additional solvent molecules but due to their severely disordered nature they cannot be structurally modelled and hence squeezed from the data set; and notably, the non-coordinated oxygen atom (O3) of nitrate is two-fold disordered with site occupation factors of 79% and 21%, respectively. The Ho(III) ion is 9-coordinated by four bridging ZW ligands, one chelating nitrate, and two chelating and bridging formates. Notably, no formic acid or salts thereof were included during MOF synthesis, probably formate was *in situ* generated upon solvothermal degradation of DMF. The carboxylate groups of the ZW ligand and the formate and nitrate anions possess each one negative charge contribute a total -4 charge toward the Ho(III) metal center and the pyridinium nitrogen making the MOF electrically neutral. The phenyl unit is partially orthogonal to the pyridinium unit within the ZW ligand, where the ∠C9-C8-N2 is 109.76°. Moreover, the two aromatic rings are slightly twisted with a dihedral ∠ of 81.7(2) ° to promote metal coordination. The shortest metal-metal distance is 4.282(3) Å, and remarkably, no solvent molecules coordinate to the metal center. Intermolecular non-

classical hydrogen bonding interactions can be found involving hydrogens of the ligand with oxygen atoms of both the nitrate and the carboxylate group as listed in **Table S2**. Also, relatively strong intermolecular aromatic π – π stacking interactions between the pyridinium rings [N2-C6-C7-C3-C4-C5] are observed with a ring center to center distance of 3.511(2) Å. The crystal structure does not belong to any standard topology setting but it is related to *gek2* topology. Taking all extensive intermolecular interactions into account, the overall crystal packing can be considered as a microporous MOF forming 1D channel pores along the crystallographic *b*-axis with pore diameters of approximately 7 Å. We recently reported a series of rare earth MOFs/coordination polymers with the same ZW ligand but none of them is isomorphous to **H1**.²¹

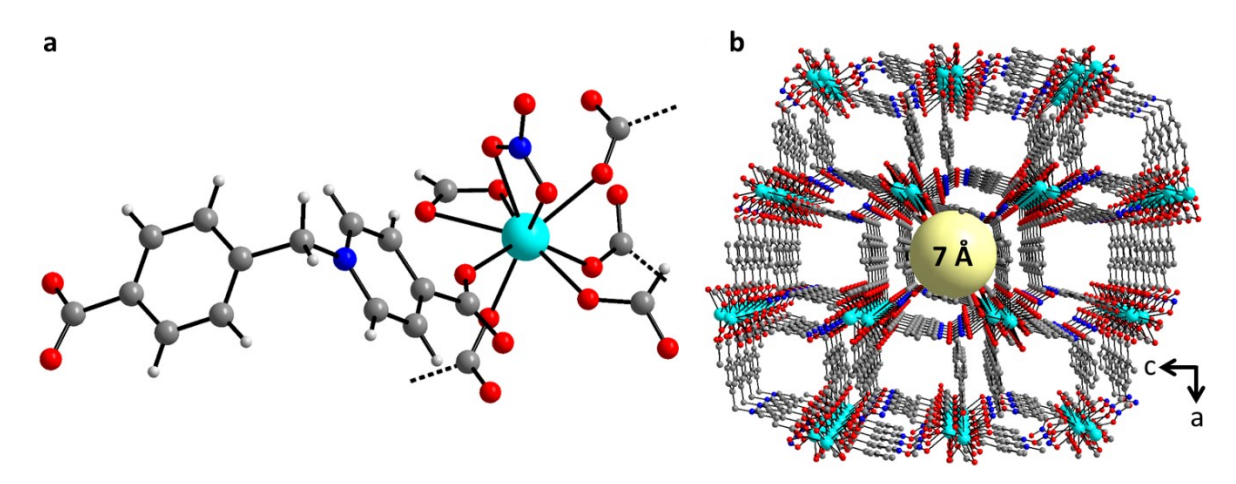


Figure 1. Crystal structure of **H1** depicting: (a) the 9-coordinate environment of Ho(III); and (b) the crystal packing with view along the crystallographic *b*-axis where the yellow spheres represent potential solvent accessible voids, hydrogen atoms are omitted for the sake of clarity.

3.3 Thermal characteristics

The thermal behavior of bulk **H1** was characterized by TGA and DTA measurements. Respective data curves are shown in **Figure 2b**. Upon heating to 260 °C, a minor mass loss step of 8.4% is observed which can be attributed to the removal of lattice solvent. Upon further heating, the MOF decomposes exothermally in a complex two-step fashion with full thermal decomposition observed at 493 °C. Follow-on experiments on probing the pore space by volumetric nitrogen adsorption isotherms were not successful probably owed to pore collapse upon thermal activation.

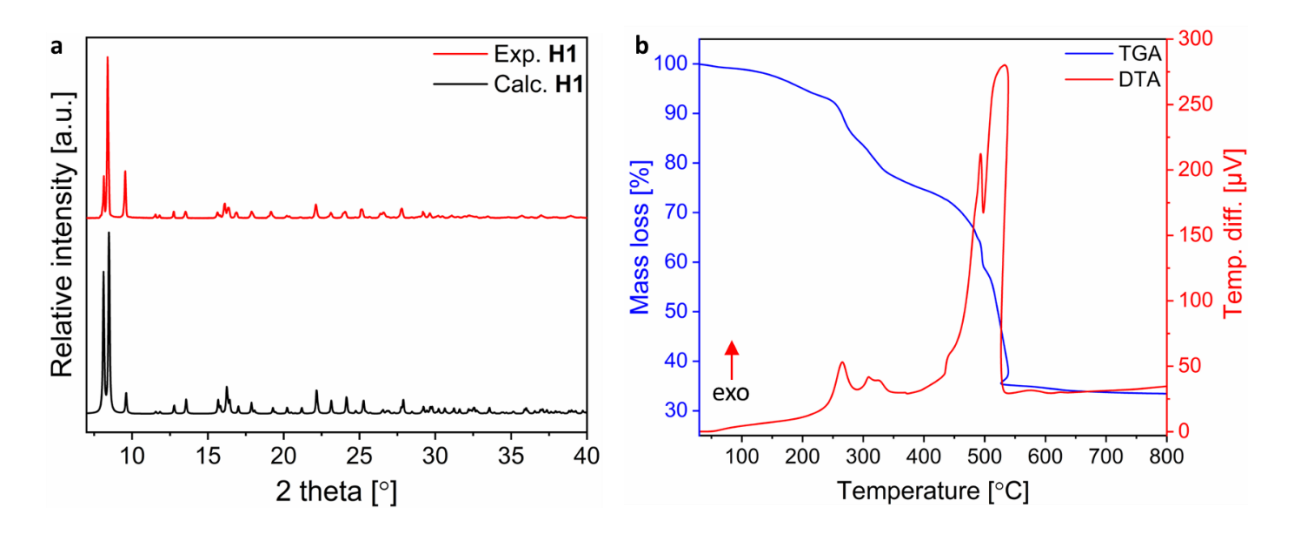


Figure 2. Bulk characterization of **H1**: (a) powder XRD pattern and (b) thermal characterization including TGA and DTA.

3.4 Unique optical feature

H1 features unique optical property as manifested by a unique color change upon varying the incident light source. Figure 3a shows that upon sunlight irradiation, the MOF appears as colorless material, while a change to pale pink is observed under fluorescent light. This unique color change is trivial in some Holmium-based salts and oxides; however, to the best of our knowledge, this feature has not been documented before in MOFs and/or coordination polymers (CPs). An extensive CCDC database search revealed 554 Ho(III)-based MOFs/CPs as of 2023, and after careful analysis of respective publications, it is evident that no similar optical behavior is documented for any of those reported materials. Table S3 lists the results of this analysis. Therefore, to the best of our knowledge, H1 is the first Ho(III)-MOF reported to feature physical color change upon changing the incident light source. It can be assumed that the pale pink color under fluorescent light is a direct result from the specific absorption of H1 in the green part of the spectrum from fluorescent light. Spectral UV-Vis absorbance data was collected to get insight into this unique optical property. As evident in Figure 3b, the UV-Vis spectrum of H1 shows the presence of a relatively sharp absorption peak in the green range at 538 nm, which reasonably overlaps the green emission peak ranging 500 to 550 nm of the fluorescent light. The resulting complementary color is pink. A partial overlap of wavelength 486 nm in the cyan range is also present with the fluorescent light source. While the complementary color is red, this overlap reinforces pink to be the dominant color. The blue and red emission peaks are insignificant and do not match the spectral bands of H1. On the other hand, in natural daylight/sunlight, H1 absorbs in the blue (452 nm), green (538 nm), and red (644 nm) regions of the spectrum resulting in an overall colorless appearance of the material.

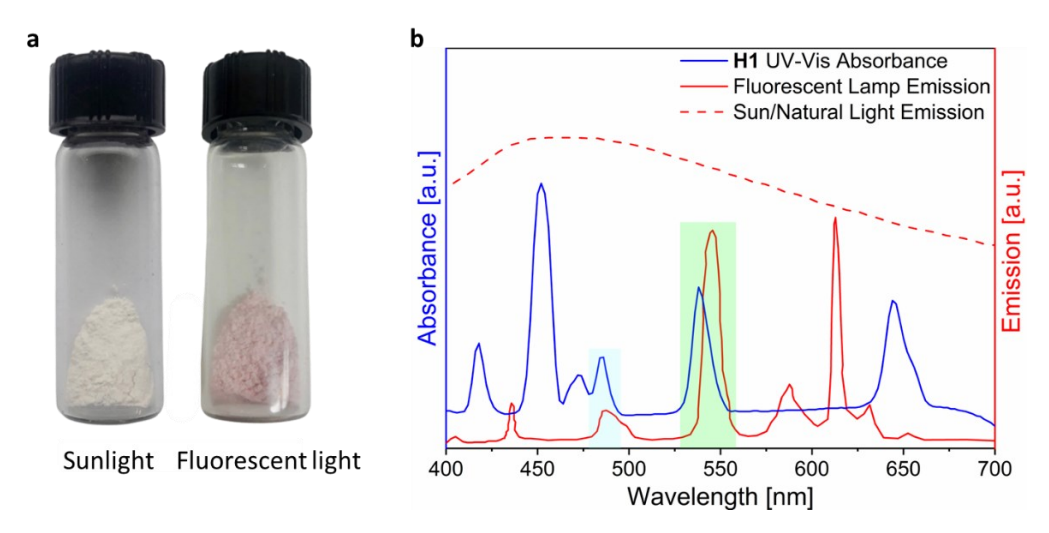


Figure 3. Optical properties showing (a) the distinct difference in color of **H1** under different incident light sources; and (b) the UV-Vis absorbance spectrum along with the emission spectra of fluorescent³⁶ and sunlight. The photoluminescence emission spectrum of **H1** is provided in ESI (**Figure S1**).

4. Conclusion

In summary, **H1** represents the first reported Holmium-based MOF showing a distinct color change upon switching the incident light source from sunlight to fluorescent light. This claim is supported by a detailed CCDC analysis of publications corresponding to Ho(III)-MOFs and CPs.

Acknowledgments

M.W. gratefully acknowledges the U.S. National Science Foundation CAREER Program (award no. DMR-1752771) for support of this work.

References

- (1) Yin, H.-Q.; Yin, X.-B. Metal–Organic Frameworks with Multiple Luminescence Emissions: Designs and Applications. *Acc. Chem. Res.* **2020**, *53* (2), 485–495. https://doi.org/10.1021/acs.accounts.9b00575.
- (2) Yin, H.-Q.; Yin, X.-B. Multi-Emission from Single Metal—Organic Frameworks under Single Excitation. *Small* **2022**, *18* (14), 2106587. https://doi.org/10.1002/sml1.202106587.
- (3) Gustafsson, M.; Bartoszewicz, A.; Martín-Matute, B.; Sun, J.; Grins, J.; Zhao, T.; Li, Z.; Zhu, G.; Zou, X. A Family of Highly Stable Lanthanide Metal—Organic Frameworks: Structural Evolution and Catalytic Activity. *Chem. Mater.* **2010**, *22* (11), 3316–3322. https://doi.org/10.1021/cm100503q.
- (4) Liu, B.; Wu, W.-P.; Hou, L.; Wang, Y.-Y. Four Uncommon Nanocage-Based Ln-MOFs: Highly Selective Luminescent Sensing for Cu2+ Ions and Selective CO2 Capture. *Chem. Commun.* **2014**, 50 (63), 8731–8734. https://doi.org/10.1039/C4CC03049D.
- (5) Zhou, J.-M.; Shi, W.; Xu, N.; Cheng, P. Highly Selective Luminescent Sensing of Fluoride and Organic Small-Molecule Pollutants Based on Novel Lanthanide Metal–Organic Frameworks. *Inorg. Chem.* **2013**, *52* (14), 8082–8090. https://doi.org/10.1021/ic400770j.

- (6) Meyer, L. V.; Schönfeld, F.; Müller-Buschbaum, K. Lanthanide Based Tuning of Luminescence in MOFs and Dense Frameworks from Mono- and Multimetal Systems to Sensors and Films. *Chem. Commun.* **2014**, *50* (60), 8093–8108. https://doi.org/10.1039/C4CC00848K.
- (7) Zhao, S.-N.; Li, L.-J.; Song, X.-Z.; Zhu, M.; Hao, Z.-M.; Meng, X.; Wu, L.-L.; Feng, J.; Song, S.-Y.; Wang, C.; Zhang, H.-J. Lanthanide Ion Codoped Emitters for Tailoring Emission Trajectory and Temperature Sensing. *Advanced Functional Materials* **2015**, *25* (9), 1463–1469. https://doi.org/10.1002/adfm.201402061.
- (8) Ma, S.; Yuan, D.; Wang, X.-S.; Zhou, H.-C. Microporous Lanthanide Metal-Organic Frameworks Containing Coordinatively Linked Interpenetration: Syntheses, Gas Adsorption Studies, Thermal Stability Analysis, and Photoluminescence Investigation. *Inorg. Chem.* 2009, 48 (5), 2072–2077. https://doi.org/10.1021/ic801948z.
- (9) Zhang, Y.; Liu, S.; Zhao, Z.-S.; Wang, Z.; Zhang, R.; Liu, L.; Han, Z.-B. Recent Progress in Lanthanide Metal—Organic Frameworks and Their Derivatives in Catalytic Applications. *Inorg. Chem. Front.* **2021**, *8* (3), 590–619. https://doi.org/10.1039/D0QI01191F.
- (10) Yan, W.; Zhang, C.; Chen, S.; Han, L.; Zheng, H. Two Lanthanide Metal–Organic Frameworks as Remarkably Selective and Sensitive Bifunctional Luminescence Sensor for Metal Ions and Small Organic Molecules. *ACS Appl. Mater. Interfaces* **2017**, *9* (2), 1629–1634. https://doi.org/10.1021/acsami.6b14563.
- (11) Li, G.-P.; Liu, G.; Li, Y.-Z.; Hou, L.; Wang, Y.-Y.; Zhu, Z. Uncommon Pyrazoyl-Carboxyl Bifunctional Ligand-Based Microporous Lanthanide Systems: Sorption and Luminescent Sensing Properties. *Inorg. Chem.* **2016**, *55* (8), 3952–3959. https://doi.org/10.1021/acs.inorgchem.6b00217.
- (12) Xie, X.-Z.; Zhang, Y.-R.; Wu, Y.-J.; Yin, X.-B.; Xia, Y. Ligand Energy Staff Gauge for Antenna Effect Study within Metal—Organic Frameworks. *J. Phys. Chem. C* **2023**, *127* (2), 1220–1228. https://doi.org/10.1021/acs.jpcc.2c07084.
- (13) Sun, Y.-Q.; Cheng, Y.; Yin, X.-B. Dual-Ligand Lanthanide Metal-Organic Framework for Sensitive Ratiometric Fluorescence Detection of Hypochlorous Acid. *Anal. Chem.* **2021**, *93* (7), 3559–3566. https://doi.org/10.1021/acs.analchem.0c05040.
- (14) Xia, Y.-D.; Sun, Y.-Q.; Cheng, Y.; Xia, Y.; Yin, X.-B. Rational Design of Dual-Ligand Eu-MOF for Ratiometric Fluorescence Sensing Cu2+ Ions in Human Serum to Diagnose Wilson's Disease. *Analytica Chimica Acta* **2022**, *1204*, 339731. https://doi.org/10.1016/j.aca.2022.339731.
- (15) Zhang, Y.-R.; Xie, X.-Z.; Yin, X.-B.; Xia, Y. Flexible Ligand for Metal-Organic Frameworks with Simultaneous Large-Pore and Antenna Effect Emission. *Chemical Engineering Journal* **2022**, *443*, 136532. https://doi.org/10.1016/j.cej.2022.136532.
- (16) Wang, X.-L.; Mu, B.; Lin, H.-Y.; Yang, S.; Liu, G.-C.; Tian, A.-X.; Zhang, J.-W. Assembly and Properties of Transition-Metal Coordination Polymers Based on Semi-Rigid Bis-Pyridyl-Bis-Amide Ligand: Effect of Polycarboxylates on the Dimensionality. *Dalton Trans.* **2012**, *41* (36), 11074–11084. https://doi.org/10.1039/C2DT30907F.
- (17) Dong, X.-Y.; Si, C.-D.; Fan, Y.; Hu, D.-C.; Yao, X.-Q.; Yang, Y.-X.; Liu, J.-C. Effect of N-Donor Ligands and Metal Ions on the Coordination Polymers Based on a Semirigid Carboxylic Acid Ligand: Structures Analysis, Magnetic Properties, and Photoluminescence. *Crystal Growth & Design* **2016**, *16* (4), 2062–2073. https://doi.org/10.1021/acs.cgd.5b01734.
- (18) Bing, Y.; Yu, M.; Hu, M. Synthesis, Structures, and Properties of Seven Transition Metal Coordination Polymers Based on a Long Semirigid Dicarboxylic Acid Ligand. *RSC Adv.* **2015**, *5* (58), 47216–47224. https://doi.org/10.1039/C5RA06012E.
- (19) Vlasyuk, D.; Łyszczek, R. Effect of Different Synthesis Approaches on Structural and Thermal Properties of Lanthanide(III) Metal—Organic Frameworks Based on the 1H-Pyrazole-3,5-Dicarboxylate Linker. *J Inorg Organomet Polym* **2021**, *31* (8), 3534–3548. https://doi.org/10.1007/s10904-021-02018-w.
- (20) Guo, X.; Zhu, G.; Li, Z.; Sun, F.; Yang, Z.; Qiu, S. A Lanthanide Metal–Organic Framework with High Thermal Stability and Available Lewis-Acid Metal Sites. *Chem. Commun.* **2006**, No. 30, 3172–3174. https://doi.org/10.1039/B605428E.

- (21) Aghamohammadi, P.; Arici, M.; Büyükgüngör, O.; Wriedt, M.; Yeşilel, O. Z. A Series of Three Dimensional Lanthanoid(III)-Metal-Organic Frameworks with Zwitterionic Linker. *Journal of Coordination Chemistry* **2021**, *74* (16), 2657–2669. https://doi.org/10.1080/00958972.2021.2001804.
- (22) Bag, P. P.; Wang, X.-S.; Cao, R. Microwave-Assisted Large Scale Synthesis of Lanthanide Metal—Organic Frameworks (Ln-MOFs), Having a Preferred Conformation and Photoluminescence Properties. *Dalton Trans.* **2015**, *44* (26), 11954–11962. https://doi.org/10.1039/C5DT01598G.
- (23) Vizuet, J. P.; Mortensen, M. L.; Lewis, A. L.; Wunch, M. A.; Firouzi, H. R.; McCandless, G. T.; Balkus, K. J. Jr. Fluoro-Bridged Clusters in Rare-Earth Metal-Organic Frameworks. *J. Am. Chem. Soc.* **2021**, *143* (43), 17995–18000. https://doi.org/10.1021/jacs.1c10493.
- (24) Czaja, M.; Bodył-Gajowska, S.; Lisiecki, R.; Meijerink, A.; Mazurak, Z. The Luminescence Properties of Rare-Earth Ions in Natural Fluorite. *Phys Chem Minerals* **2012**, *39* (8), 639–648. https://doi.org/10.1007/s00269-012-0518-8.
- (25) Du, L.; Zhou, L.-Z.; Ma, Y.-L.; Wang, Y.-N.; Wang, D.-W.; Zhao, Q.-H. Synthesis, Structures, and Photoluminescence Properties of Five Novel Zinc(II) and Cadmium(II) Coordination Polymers Based on Different Zwitterionic Pyridine Ligands. *Zeitschrift für anorganische und allgemeine Chemie* **2017**, *643* (24), 2116–2123. https://doi.org/10.1002/zaac.201700151.
- (26) Bruker (2001) SADABS Bruker AXS Inc., Madison, Wisconsin, USA.
- (27) Sheldrick, G. M. SHELXT Integrated Space-Group and Crystal-Structure Determination. *Acta Cryst A* **2015**, *71* (1), 3–8. https://doi.org/10.1107/S2053273314026370.
- (28) Sheldrick, G. M. Crystal Structure Refinement with SHELXL. *Acta Cryst C* **2015**, 7*I* (1), 3–8. https://doi.org/10.1107/S2053229614024218.
- (29) Spek, A. L. Structure Validation in Chemical Crystallography. *Acta Cryst D* **2009**, *65* (2), 148–155. https://doi.org/10.1107/S090744490804362X.
- (30) Bruno, I. J.; Cole, J. C.; Edgington, P. R.; Kessler, M.; Macrae, C. F.; McCabe, P.; Pearson, J.; Taylor, R. New Software for Searching the Cambridge Structural Database and Visualizing Crystal Structures. *Acta Crystallographica Section B* **2002**, *58* (3–1), 389–397. https://doi.org/10.1107/S0108768102003324.
- (31) Aghamohammadi, P.; Büyükgüngör, O.; Arıcı, M.; Wriedt, M.; Yeşilel, O. Z. Synthesis and Characterization of Cerium(III), Praseodymium(III), Gadolinium(III) and Erbium(III) Coordination Polymers with Zwitterionic Ligand. *Journal of Molecular Structure* **2022**, *1250*, 131876. https://doi.org/10.1016/j.molstruc.2021.131876.
- (32) Wang, K.-M.; Du, L.; Ma, Y.-L.; Zhao, J.-S.; Wang, Q.; Yan, T.; Zhao, Q.-H. Multifunctional Chemical Sensors and Luminescent Thermometers Based on Lanthanide Metal—Organic Framework Materials. *CrystEngComm* **2016**, *18* (15), 2690–2700. https://doi.org/10.1039/C5CE02367J.
- (33) Chen, M.; Chen, M.-Z.; Zhou, C.-Q.; Lin, W.-E.; Chen, J.-X.; Chen, W.-H.; Jiang, Z.-H. Towards Polynuclear Metal Complexes with Enhanced Bioactivities: Synthesis, Crystal Structures and DNA Cleaving Activities of CuII, NiII, ZnII, CoII and MnII Complexes Derived from 4-Carboxy-1-(4-Carboxybenzyl) Pyridinium Bromide. *Inorganica Chimica Acta* **2013**, *405*, 461–469. https://doi.org/10.1016/j.ica.2013.02.008.
- (34) Bhuvaneswari, N.; Dai, F.-R.; Chen, Z.-N. Sensitive and Specific Guest Recognition through Pyridinium-Modification in Spindle-Like Coordination Containers. *Chemistry A European Journal* **2018**, *24* (25), 6580–6585. https://doi.org/10.1002/chem.201705210.
- (35) Bai, Z.; Wang, Y.; Liu, W.; Li, Y.; Xie, J.; Chen, L.; Sheng, D.; Diwu, J.; Chai, Z.; Wang, S. Significant Proton Conductivity Enhancement through Rapid Water-Induced Structural Transformation from a Cationic Framework to a Water-Rich Neutral Chain. *Crystal Growth & Design* **2017**, *17* (7), 3847–3853. https://doi.org/10.1021/acs.cgd.7b00469.
- (36) Kim, S.; Jahandar, M.; Jeong, J. H.; Lim, D. C. Recent Progress in Solar Cell Technology for Low-Light Indoor Applications. *Current Alternative Energy 3* (1), 3–17.